Computer simulation of an unconfined liquid crystal film

Stuart J. Mills,[1] Christopher M. Care,[1] Maureen P. Neal,[2] and Douglas J. Cleaver[1]
[1]*Materials Research Institute, Sheffield Hallam University, Pond Street, Sheffield S1 1WB, United Kingdom*
[2]*School of Mathematics and Information Sciences, Coventry University, Coventry CV1 5FB, United Kingdom*
(Received 30 April 1998)

We present results from a molecular dynamics simulation of an unconfined Gay-Berne film in equilibrium with its own saturated vapor. The parametrization and temperature range used are based upon the results of preliminary Gibbs ensemble investigations, which show the existence of bulk liquid-vapor and nematic-vapor coexistence. This parametrization is found to induce a preferred molecular alignment in the nematic film perpendicular to the liquid-vapor interface, in contrast to work on similar systems showing planar alignment. At slightly higher temperatures the nematic phase is wet by the isotropic, displaying an intermediate ordering regime in which the film is comprised of several short-lived nematic domains. This behavior has been analyzed using orientational correlation functions, and shown to be associated with a decoupling of the planar and perpendicular nematic ordering. The interfacial surface tension behavior has also been evaluated, and shown to be consistent with theoretical predictions for systems displaying isotropic wetting. [S1063-651X(98)14509-9]

PACS number(s): 61.30.Gd, 61.30.Cz, 68.10.Cr, 68.15.+e

I. INTRODUCTION

The surface anchoring properties of liquid crystals are crucial in determining the stability and orientation of the phases adopted in device geometries. A number of theoretical and experimental studies have been conducted regarding these effects, and phenomenological treatments [1,2] have shown qualitative agreement with trends observed experimentally [3]. However, the number of different effects at work over a wide range of length scales, coupled with the multitude of possible behaviors, makes a complete understanding of these systems a considerable challenge. The observation that subtle changes in intermolecular and molecule-substrate interactions can lead to notable changes in the bulk behavior suggests that this is a particularly suitable area for investigation by computer simulation.

The study of anchoring at the free liquid crystal-vapor interface is of importance both in its own right and as a reference for fully confined systems. The presence of an interface with no fixed barrier holding it in place allows particular attention to be focused on the effect of bond-breaking symmetry upon the system. A surprisingly rich phase behavior is found at the interface between a nematic liquid and its own saturated vapor, including various induced orientations at the interface as well as both partial and complete wetting regimes and anomalous surface tension dependence.

Early theoretical work concentrated on phenomenological descriptions, but in the past 15 years molecular theories have made significant progress. A number of papers [4–6] have been published in which a generalized van der Waals theory [7], based on a spherical harmonic expansion of the anisotropic attractive component of the intermolecular interaction potential, has been used to analyze the wetting and alignment properties of the liquid-vapor interface, both above and below the vapor-isotropic-nematic (V-I-N) triple point temperature. These show that appropriate choices of the various expansion terms can yield either perpendicular, parallel, or oblique alignment at the interface. A direct mapping of these terms onto physical interactions is not straightforward; the leading second-order term (which is the first term that couples the translational and rotational degrees of freedom, and thus gives rise to a nontrivial surface behavior) induces homeotropic alignment for prolate molecules, and planar for oblate ones. The next second-order term, which usually has a weaker influence at the free interface, has the opposite effect. Oblique alignment results when there is near cancellation of these competing terms, allowing higher-order terms to become relevant. Recently the use of a spherical hard core within this theory has been called into question [8], casting doubt over some of its predictions for highly anisotropic systems. However, the general trends observed are still thought to be valid.

A related paper [9], which employs explicit expansions of a range of parametrizations of the Gay-Berne (GB) potential [10,11], found that perpendicular alignment should arise in such systems. Conversely, studies based on perfectly ordered systems with ellipsoidally symmetric intermolecular interactions [12] predict parallel interfacial orientation. This apparent inconsistency is explained by noting [9] the considerable differences between the GB form and its predecessor, the Berne-Pechukas potential [13], which is more consistent with the ellipsoidally symmetric potentials considered in Ref. [12].

Aside from considerations of induced orientation, the wetting behavior of these systems in the vicinity of the triple point is also predicted to depend sensitively upon the terms in the molecular model used. In summary, it has been found that increasing the magnitude of the alignment-inducing terms favors nematic wetting of the isotropic phase [6,14], as would be expected intuitively. A change from partial to complete wetting occurs as these terms are increased above a threshold value, while, for sufficiently small values, isotropic wetting of the nematic phase (or surface disordering) is predicted.

The behavior of the surface tension γ in this region has been linked with the differing wetting regimes. Normally, surface tension decreases with increasing temperature, reaching a value of zero at the liquid-vapor critical point. Theo-

retical treatments of systems with disordering interfaces (i.e., showing isotropic wetting) show this trend with an additional negative discontinuity at the nematic-isotropic transition. However, for surface ordering systems, an *increase* in the surface tension with temperature on either one or both sides of the transition has been predicted, along with either a positive or negative discontinuity at the transition [5,8].

One of the first experimental investigations of free nematic surfaces looked at the surface alignment using a light reflection technique. From this, it was found that *p*-azoxyanisole (PAA) favors planar ordering, whereas 4-methoxybenzylidene-4′-butylaniline (MBBA) prefers an oblique state, the temperature-dependent tilt varying from 10 to 22° with respect to the surface normal [15]. Subsequent work confirmed this result for PAA [16] and showed that MBBA in fact undergoes a transition from tilted to homeotropic alignment at a temperature slightly below the *V-I-N* triple point [17]. Studies of another common class of liquid crystal molecules, the cyanobiphenyls, showed perpendicular alignment at the free surface for 5, 6, 7, and 8 CB [18]. This type of behavior was also seen for 8-oxy cyanobiphenyl (OCB) [19]. It is worth stressing that molecular theories are able to model all of these diverse behaviors.

Direct studies of wetting phenomena in liquid crystal systems have concentrated on order-enhancing interfaces. Reflection ellipsometry work on the cyanobiphenyls [18] showed nematic wetting of the isotropic free surface, this wetting changing from partial to complete with increase in molecular length (5 CB partial; 6, 7, and 8 CB complete). This is in good agreement with theoretical predictions of increased nematic wetting ability with an increase in the degree of molecular anisotropy. Furthermore, a study of the surface tension behavior for these systems [20] showed the expected trend for nematic wetting: a region of positive $\partial\gamma/\partial T$ and a (local) maximum in $\gamma(T)$ in the isotropic phase. More recently, prewetting transitions and a prewetting critical point have been observed at the free surfaces of various benzoic acid oxyphenylester derivatives [21]. These ellipsometric studies have all shown enhanced orientational order at the surfaces.

It is much harder to find examples of isotropic wetting in the literature, but it is possible to infer such through observation of appropriate surface tension behavior. In particular, an early study of *p*-anisaldazine and MBBA [22] showed a negative $\partial\gamma/\partial T$ and a negative discontinuity in $\gamma(T)$ at the nematic-isotropic (N-I) transition, implying a surface disordering effect [23].

Early simulation studies of these systems were restricted, by the considerable run times required, to the use of Lebwohl-Lasher–type lattice models. These considered a nematic film between two fixed walls [24–26], whose nature was expressed in terms of a modified exchange constant. For a ''free'' surface (i.e., an exchange constant of zero) this model was found to exhibit orientational disorder at its surfaces, no preferred orientation being induced. This result is unsurprising, given the lack of density variation inherent in the Lebwohl-Lasher model, and its degeneracy to en-masse rotation of all spins. Despite these shortfalls, simulations of this model were able to measure $\gamma_{N\text{-}I}$ and to confirm the existence of a critical film thickness at which the first-order N-I transition vanishes [26].

Recently, two independent groups [27,28] have simulated a more realistic nematic-vapor system, using the well-established GB potential [10]. Here, the lattice restriction is lifted so that translational and rotational degrees of freedom are coupled. The parametrization used in both of these studies had previously been shown to display bulk nematic-vapor coexistence using the Gibbs ensemble Monte Carlo (GEMC) technique [29]. Both groups found that, for this parametrization, the free interfaces enhance orientational order and induce a director lying in a plane parallel to the interface.

In this paper, we present results from a similar study but employ a significantly different parametrization of the GB potential. With this modified parametrization, the interfaces are shown to be disordering, inducing a different surface orientation and resulting in a rather more complicated behavior through the ordering transition. In the next section, we briefly describe the model used. In Sec. III we present details of the GEMC and molecular dynamics (MD) simulations performed, along with relevant analysis. Finally, we discuss the results and draw our conclusions.

II. GAY-BERNE POTENTIAL

The GB potential, essentially an anisotropic form of the classic Lennard-Jones 12-6 potential, has been shown to display a variety of liquid crystalline phases [30,31]. In the GB potential, the interaction between two particles is given by

$$U_{ij}(\hat{\mathbf{u}}_i,\hat{\mathbf{u}}_j,\hat{\mathbf{r}}_{ij}) = 4\epsilon(\hat{\mathbf{u}}_i,\hat{\mathbf{u}}_j,\hat{\mathbf{r}}_{ij})\left[\left(\frac{\sigma_0}{r_{ij}-\sigma(\hat{\mathbf{u}}_i,\hat{\mathbf{u}}_j,\hat{\mathbf{r}}_{ij})+\sigma_0}\right)^{12} - \left(\frac{\sigma_0}{r_{ij}-\sigma(\hat{\mathbf{u}}_i,\hat{\mathbf{u}}_j,\hat{\mathbf{r}}_{ij})+\sigma_0}\right)^{6}\right], \tag{1}$$

where $\hat{\mathbf{u}}_i$, $\hat{\mathbf{u}}_j$, and $\hat{\mathbf{r}}_{ij}$ are unit vectors describing the orientations of the two particles and the interparticle vector. Except where otherwise stated, σ_0 and ϵ_0 (the well-depth minimum for the cross configuration) are taken to be unity. More information on the various terms can be found elsewhere [10], but it should be noted that the potential requires four parameters to be explicitly selected: κ and κ', which, respectively, define the shape and well-depth anisotropies, and μ and ν, which adjust the relative strengths of various intermolecular interactions. Variation of these parameters can lead to notable changes in the phase behavior of the model [29,30,32], such that it is possible for the GB potential to exhibit a number of different types of liquid crystalline behavior.

In the nematic-vapor studies mentioned earlier [27,28], the parametrization $\kappa=3.0$, $\kappa'=1.0$, $\mu=2.0$, and $\nu=1.0$ was used, following GEMC results [29] that showed this system to display stable nematic-vapor coexistence. In the current study, the values $\kappa=2.0$, $\kappa'=5.0$, $\mu=1.0$, $\nu=2.0$ have been employed. As pointed out by Luckhurst, Stephens, and Phippen [30], these alternative values of μ and ν result in deeper well depths for parallel orientations of the particles. A similar choice of κ, κ', μ, and ν was found to be necessary to create radially layered structures in simulations of a polymer dispersed liquid crystal system [33]. Using this ''stronger'' μ and ν, we made an attempt to locate the liquid-vapor region for $\kappa=3.0$, $\kappa'=5.0$, but no stable coexistence could be found. Guided by the results of Brown *et al.* [32],

an attempt to remedy this, by reducing the shape anisotropy ($\kappa=3.0$ to $\kappa=2.0$) while keeping the other parameters unchanged, did yield the desired coexistence (as demonstrated in the following section). Note—in both of the following sets of simulations, the intermolecular potential was truncated and shifted at a distance $r_c=4\sigma_0$.

III. SIMULATION DETAILS AND RESULTS

The liquid-vapor coexistence behavior of the model was established using the GEMC technique. The results of these simulations were subsequently used as the basis for a detailed study of the liquid-vapor interface, performed using standard MD methods.

A. GEMC simulations

The GEMC technique was developed in the late 1980s specifically to enable the direct simulation of fluid phase equilibria. More details can be found in the appropriate publications [34]; essentially the technique involves simulating the two phases in separate, but coupled, boxes, and allowing three types of MC move to ensure that the boxes remain in thermal, mechanical and chemical equilibrium with one another. Both boxes are surrounded by their own periodic images so that there need be no interfaces between the two phases; the results can therefore be regarded as a measure of bulk coexistence (subject to finite size effects).

In practice, a system simulated in a coexistence region with the GEMC technique evolves so that each box contains just one of the coexisting phases. The underlying driving force for this is the system's desire to avoid the energetic cost of establishing an interface. Since the boxes are not in direct physical contact, it can do this by allocating a separate phase to each.

Our simulations were started using two independent isotropic configurations of 256 particles, each equilibrated at high temperature and low density using standard MC. Both were then compressed to a reduced number density ρ of 0.1, a value known to be in the coexistence region for other GB systems [29]. The additional GEMC moves were then switched on, to couple the two boxes, and the density in each box was monitored. The temperature of the simulation was decreased, in fairly large steps, until clear phase coexistence was observed. Further points on the coexistence curve were then obtained by slowly cooling, the initial configuration at each new temperature being the final configuration obtained at the previous point. Typically, relatively small equilibration runs of 10 000 MC sweeps were required to achieve stability, the densities and order parameters reported being obtained from production runs of 20 000 sweeps. One attempted box-volume change move was made after each sweep of the system. The frequency of particle interchange moves was varied so as to achieve an overall average of 1–3 % of the particles changing boxes per MC sweep, in accord with the original prescription of Panagiotopoulos [34]. This was achieved without recourse to orientationally biased insertion techniques; we attribute this to the relatively small degree of shape anisotropy being used. Further information on performing GEMC simulations of Gay-Berne systems can be found elsewhere [29].

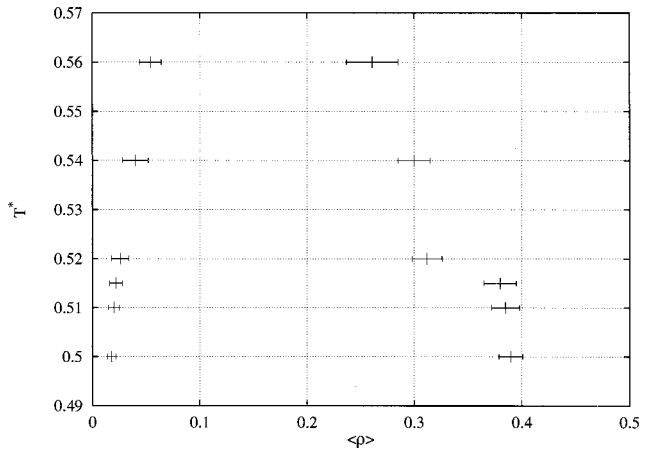

FIG. 1. Phase diagram obtained from GEMC simulations. Points represent coexisting densities ($\langle\rho_l\rangle$ and $\langle\rho_v\rangle$) at each temperature (T^*). The density is in units of σ_0^{-3}.

In this and subsequent sections, we use a reduced temperature, $T^*=k_BT/\epsilon_0$, where k_B is the Boltzmann constant, and measure nematic order using the run average of

$$P_2=\frac{1}{N}\sum_{i=1}^{N}\left[\tfrac{3}{2}(\hat{\mathbf{u}}_i\cdot\hat{\mathbf{d}})^2-\tfrac{1}{2}\right], \tag{2}$$

where $\hat{\mathbf{d}}$ is the system director [defined as the orientation that maximizes the right-hand side of Eq. (2)].

The results of our GEMC simulations are summarised in Fig. 1 and Table I. From Fig. 1, we observe characteristic liquid-vapor coexistence behavior for $0.560\geqslant T^*\geqslant 0.520$, the two boxes developing liquid and vapor densities, ρ_l and ρ_v, respectively. The discontinuity in the density apparent on the liquid side of the coexistence envelope at $T^*\simeq 0.515$ is consistent with a phase transition to an orientationally ordered fluid. The liquid-phase $\langle P_2\rangle$ data given in Table I confirm this transition from isotropic to nematic, both phases proving stable in coexistence with the saturated vapor. At the temperatures studied with GEMC, no smectic structure was found in the liquid phase. The rather large density discontinuity we have observed at the *I*-*N* transition is thought to arise due to the small length-to-breadth ratio of the particles used.

B. Direct simulations of an unconfined liquid film

Guided by our GEMC results, the interfacial properties of a thin film of 1626 GB particles have been investigated around the *V*-*I*-*N* triple point, using single-box simulations

TABLE I. Nematic order parameter, as measured in the liquid box, in the GEMC simulations.

T^*	$\langle P_2\rangle$
0.560	0.086
0.540	0.099
0.520	0.085
0.515	0.685
0.510	0.749
0.500	0.746

TABLE II. Details and results of MD simulations. All observables were averaged over production runs of 250 000 timesteps. Error estimates, given in parentheses, correspond to the last two significant figures. Equilibration run lengths, in thousands of time steps, are shown in the last column.

T^*	$\langle U\rangle$	$\langle\rho_v\rangle$	$\langle\rho_l\rangle$	$\langle P_2\rangle$	$\langle Q_{zz}\rangle$	$\langle Q_{zz}\rangle/\langle P_2\rangle$	Equil.
0.520	−2.262(43)	0.035	0.309	0.041(14)	0.005(24)	0.122	200
0.500	−2.457(42)	0.024	0.329	0.047(18)	0.004(27)	0.085	200
0.490	−2.558(36)	0.020	0.337	0.056(22)	0.004(29)	0.071	200
0.485	−2.630(34)	0.018	0.343	0.053(19)	0.002(28)	0.038	200
0.480	−2.701(38)	0.013	0.346	0.060(23)	0.003(29)	0.050	200
0.475	−2.750(59)	0.016	0.353	0.126(58)	−0.022(47)	−0.175	350
0.473	−2.966(06)	0.015	0.369	0.286(53)	−0.130(37)	−0.455	350
0.470	−3.243(06)	0.013	0.382	0.461(38)	−0.016(75)	−0.035	1200
0.465	−3.412(52)	0.012	0.397	0.549(28)	0.333(84)	0.607	500
0.460	−3.604(46)	0.011	0.406	0.626(23)	0.577(32)	0.922	400
0.455	−3.687(57)	0.009	0.408	0.643(27)	0.597(52)	0.928	300
0.450	−3.786(42)	0.008	0.412	0.676(18)	0.634(39)	0.938	200
0.445	−3.887(45)	0.008	0.418	0.695(20)	0.591(68)	0.850	200
0.440	−5.212(31)	0.007	0.475	0.889(04)	0.819(08)	0.921	350

in the temperature region $0.460 \leqslant T^* \leqslant 0.550$. Initial simulations using one-box MC proved to be inefficient, due to the slow and incoherent reorientation of the ordered domains; constant *NVT* MD was employed instead. The temperature was kept constant by rescaling the velocities at each time step, this being fixed at $\delta t = 0.0015(m\sigma_0^2/\epsilon_0)^{1/2}$.

An initial starting configuration was generated by taking an equilibrated isotropic configuration at $T^* = 0.550$ and $\rho = 0.35$ in a 1:1:3 box and sandwiching it with vapor on both sides in the z direction using a similarly equilibrated vapor configuration generated at the same temperature but a much lower density. This resulted in a film with two liquid-vapor interfaces, each in an x-y plane, occupying the middle half of a 1:1:6 box ($11.4\sigma_0 : 11.4\sigma_0 : 68.1\sigma_0$), with fully periodic boundary conditions. The system was allowed to equilibrate at this temperature until the interfaces had stabilized. It was then gently cooled, being allowed to equilibrate at each temperature such that each of the measured quantities (particularly the profiles) had stabilized. Equilibration times are shown in Table II along with averages for various observables, these being compiled over 250 000-time-step production runs.

In order to measure the orientational order with respect to the normal to the interface planes, we have calculated

$$Q_{zz} = \frac{1}{N}\sum_{i=1}^{N}\left[\tfrac{3}{2}u_{i,z}^2 - \tfrac{1}{2}\right] \tag{3}$$

as well as measuring the nematic order parameter, P_2. P_2 varies between zero for totally disordered (isotropic) regions, and unity for perfectly aligned orientational order. In practice, nematic regions might be expected to have a P_2 value between 0.4 and 0.7. Q_{zz} takes similar values to P_2, but measures orientational order with respect to the fixed lab-frame z axis. Since in this system the z axis is normal to the interfaces, Q_{zz} can be used to determine the extent of any surface-induced alignment. In practice, Q_{zz} is restricted by P_2 (i.e., it can never be greater in magnitude) so the ratio Q_{zz}/P_2 is useful in determining the alignment for systems displaying intermediate orientational order. While both of these quantities were measured for the system as a whole, the values obtained are considered to be a reasonable indicator

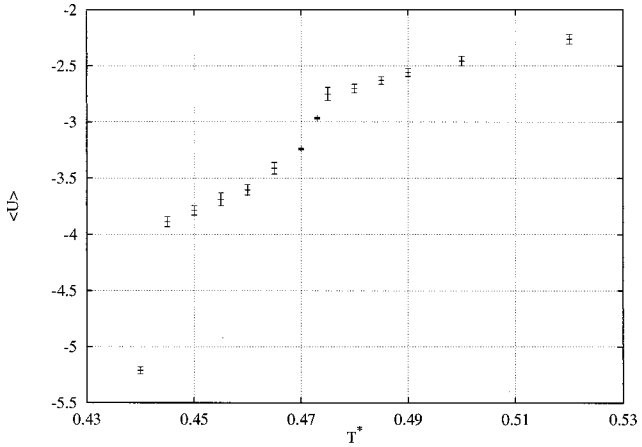

FIG. 2. Run averaged potential energy $\langle U\rangle$ (with error bars) as a function of temperature. The potential energy is in units of ϵ_0.

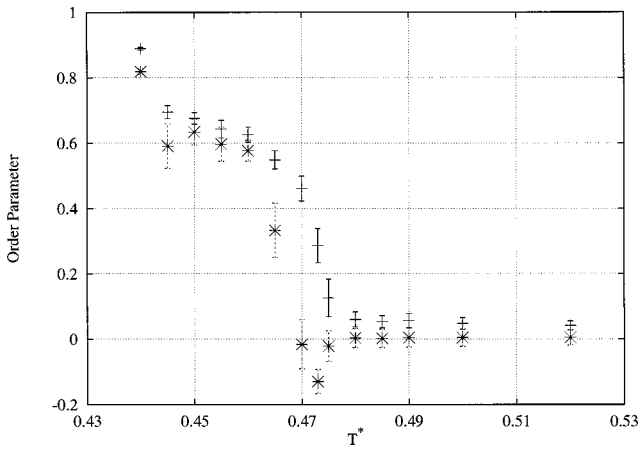

FIG. 3. Run-averaged order parameter values (with error bars) as a function of temperature $\langle P_2\rangle$ (+); $\langle Q_{zz}\rangle$ (×).

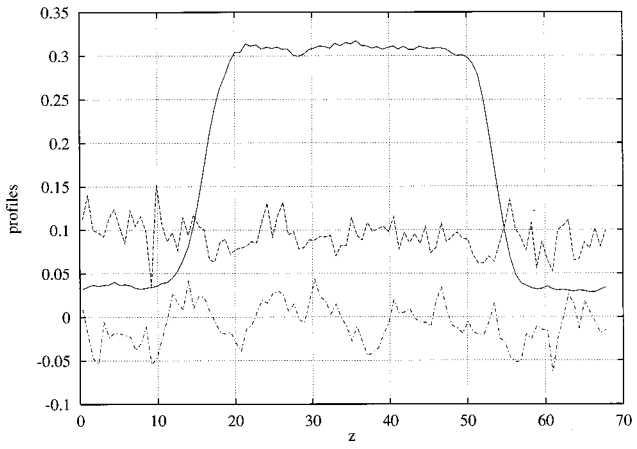

FIG. 4. Run-averaged profiles at $T^*=0.520$: $\langle\rho(z)\rangle$ (solid line); $\langle P_2(z)\rangle$ (dashed line); $\langle Q_{zz}(z)\rangle$ (dash-dot line). The z coordinate is in units of σ_0 and the density in units of σ_0^{-3}.

of the order in the liquid film, as many more particles reside in the liquid than in the vapor.

Since the primary aim of this study was to investigate the orientational effects across the width of the film, various observables were profiled across the box by dividing the system into 100 strips in the z direction and calculating the appropriate quantities for the molecules in each strip. These include the density $\rho(z)$ and the two orientational order parameters $P_2(z)$ and $Q_{zz}(z)$. The $P_2(z)$ values were renormalized using a modified eigenvalue calculation presented previously [35], in order to reduce the tendency for small numbers of molecules in the vapor phase to give misleadingly high values. Each average density profile was fitted to a double hyperbolic tangent form (i.e., one for each interface), from which the liquid and vapor densities, $\langle\rho_l\rangle$ and $\langle\rho_v\rangle$, were obtained. Two other quantities measured for each slice were the normal and tangential components of the pressure tensor, defined by [36]

$$p_N(z)=\rho(z)T^*-\frac{1}{2V_c}\sum_{i,j}^{(k)} z_{ij}\frac{\partial U_{ij}}{\partial z_{ij}}, \tag{4}$$

$$p_T(z)=\rho(z)T^*-\frac{1}{4V_c}\sum_{i,j}^{(k)}\left[x_{ij}\frac{\partial U_{ij}}{\partial x_{ij}}+y_{ij}\frac{\partial U_{ij}}{\partial yij}\right], \tag{5}$$

where V_c is the volume of each slice and the symbol (k) means that the summation is restricted to pairs of molecules of which at least one is in the corresponding slice. The surface tension γ was then calculated from these by numerical integration according to the expression

$$\gamma=\int_{z_v}^{z_l}[p_N(z)-p_T(z)]dz, \tag{6}$$

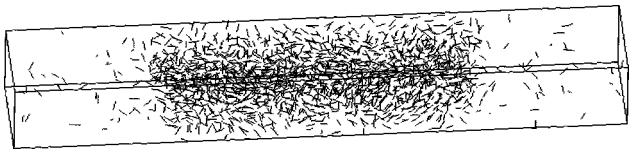

FIG. 5. Configuration snapshot at $T^*=0.520$. Particles are represented by a line of length $1\sigma_0$ along the main symmetry axis.

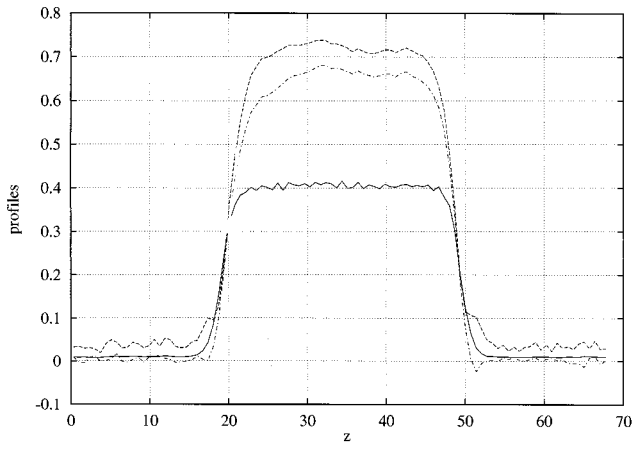

FIG. 6. Run-averaged profiles at $T^*=0.455$: $\langle\rho(z)\rangle$ (solid line); $\langle P_2(z)\rangle$ (dashed line); $\langle Q_{zz}(z)\rangle$ (dash-dot line). The z coordinate is in units of σ_0 and the density in units of σ_0^{-3}.

where the limits of integration refer to z values in the bulk liquid and vapor phases far from the interface. In practice, the integration was performed over both interfaces present in the system, and a value for γ obtained by averaging over the two.

1. Orientational order

Results for the run averaged potential energy per particle $\langle U\rangle$ and the orientational order parameters are shown in Figs. 2 and 3. The potential energy curve shows clear linear regions at high and low temperatures, but is distinctly nonlinear for the intermediate temperature regime $0.460\leqslant T^*\leqslant 0.475$. Also, a sharp discontinuity is apparent at $T^*\simeq 0.440$. The order parameter data indicate that for $T^*\geqslant 0.475$, the film remains in the isotropic phase. Inspection of the system profiles and configuration snapshot for $T^*=0.520$ (Figs. 4 and 5) confirms this. For $0.445\leqslant T^*\leqslant 0.460$, both the overall nematic order parameter and $\langle Q_{zz}\rangle$ adopt values of about 0.6, suggesting a nematic phase aligned normal to the free interfaces. Again, this situation is verified by the system profiles and configuration snapshot for $T^*=0.455$ (Figs. 6 and 7). The profiles show that, at this temperature, the film is a nematic monodomain, the orientational order penetrating all the way out to both liquid-vapor interfaces. The ratio Q_{zz}/P_2 both for this profile and for the run-averaged values given in Table II is consistently above 0.9, indicating that the orientation of the nematic monodomain is preferentially aligned normal to the free interfaces throughout the temperature range $0.450\leqslant T^*\leqslant 0.460$.

We note that the degree of perpendicular order indicated by the ratio of order parameters reaches a maximum, at $T^*\simeq 0.455$. Upon further cooling, this ratio decreases slightly, before the system undergoes what appears to be a first-order phase transition at $T^*=0.440$. The high orientational order

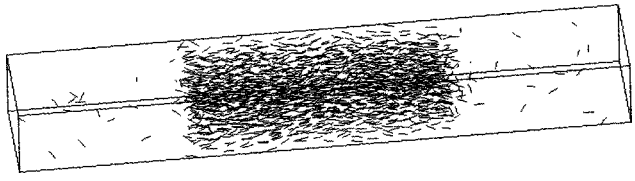

FIG. 7. Configuration snapshot at $T^*=0.455$. Particles are represented by a line of length $1\sigma_0$ along the main symmetry axis.

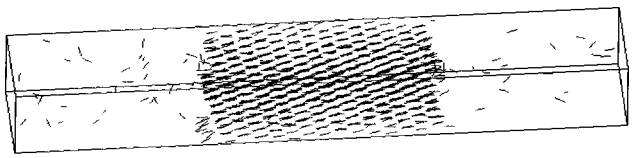

FIG. 8. Configuration snapshot at $T^*=0.440$. Particles are represented by a line of length $1\sigma_0$ along the main symmetry axis.

parameters at this temperature indicate a highly ordered system and a layered structure is clearly visible from the appropriate snapshot (Fig. 8), with hexagonal packing evident in the layers. This structure appears to be a crystalline solid the layers of which are slightly tilted with respect to the interface normal, contrary to the preferred direction in the nematic phase. It is suggested that this is due to the box dimensions originally chosen being incommensurate with the hexagonal layers, stopping the system from ordering perpendicularly and forcing it to adopt a tilted arrangement. The boundary conditions also explain the apparent partial layers observable at the interfaces in Fig. 8. Had the box dimensions been allowed to change (while keeping the overall volume constant) the system would have found its truest lowest energy state with perpendicular ordering in the crystal phase. This also explains why the degree of perpendicular ordering starts to decrease in the nematic phase: as the crystal phase is approached, competition develops between the interfacial and boundary-condition contributions to the preferred system orientation.

We note that the development of nematic order within the film is not at all clean cut. First to consider is the prenematic ordering at $T^*=0.475$ and 0.473. Here, the nematic order parameter $\langle P_2\rangle$ shows an increase, though not enough to indicate a nematic phase. The associated small/negative values of $\langle Q_{zz}\rangle$ seem rather contradictory, given that the final stable nematic has a positive $\langle Q_{zz}\rangle$. This can be partially explained by looking at run-averaged profiles at these two temperatures (Figs. 9 and 10, respectively). These show reduced orientational order at the interfaces, suggesting (incorrectly) that a single domain of nematic is seeded at the center of the film, and widens slowly with reducing temperature. The negative regions in the associated $\langle Q_{zz}(z)\rangle$ profiles give

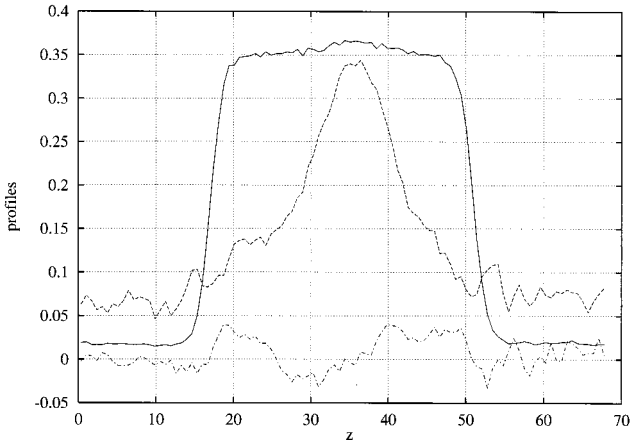

FIG. 9. Run-averaged profiles at $T^*=0.475$: $\langle\rho(z)\rangle$ (solid line); $\langle P_2(z)\rangle$ (dashed line); $\langle Q_{zz}(z)\rangle$ (dash-dot line). The z coordinate is in units of σ_0 and the density in units of σ_0^{-3}.

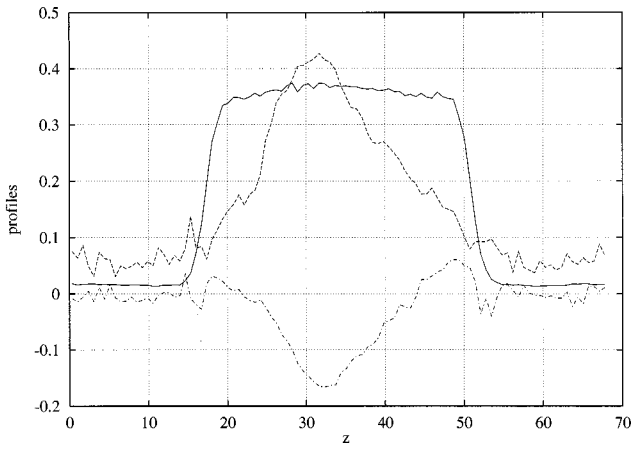

FIG. 10. Run-averaged profiles at $T^*=0.473$: $\langle\rho(z)\rangle$ (solid line); $\langle P_2(z)\rangle$ (dashed line); $\langle Q_{zz}(z)\rangle$ (dash-dot line). The z coordinate is in units of σ_0 and the density in units of σ_0^{-3}.

a weak indication that this nematic domain is tilted with respect to the z axis. This could be attributed to a preferred alignment associated with the implicit nematic-isotropic interfaces. We note, however, that the values of the all particle observable $\langle Q_{zz}\rangle$ shown in Fig. 3 are zero to within error estimates for all but one $T^*\geqslant 0.470$. Further analysis leads us to conclude that a slowly changing multidomain structure is adopted by the system in this intermediate temperature regime, no clearly stable preferred orientation being observed.

As first evidence of this multi-domain structure, we present, in Fig. 11, time series of P_2 and Q_{zz} obtained from the long equilibration run at $T^*=0.470$. Here, the nematic order is found to penetrate virtually all the way up to the interfaces and so perpendicular ordering might have been expected. In fact, the Q_{zz} data show long negative (i.e., tilted) and positive (i.e., perpendicular) periods before equilibrating to the region $-0.2\leqslant Q_{zz}\leqslant 0.2$. Even in this equilibrated period, oscillations are seen to occur on time scales of order 10^5 time steps. Animations of the runs in the intermediate temperature regime (i.e., $0.460\leqslant T^*\leqslant 0.475$) indicate that at any instant, far from there being a single central nematic domain, the system typically comprises a series of competing domains. These are commonly seeded near to the film

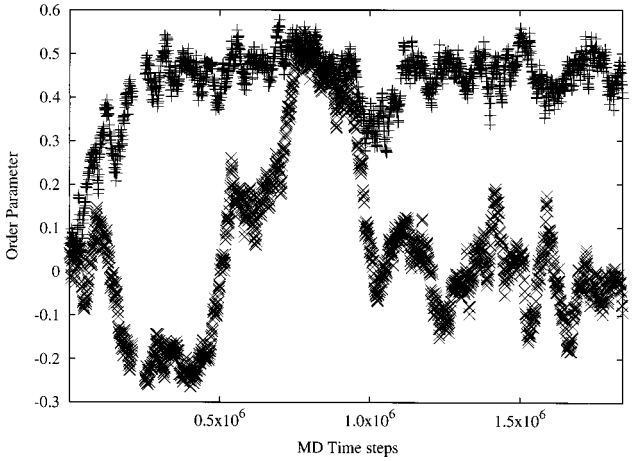

FIG. 11. Instantaneous order parameter values for MD equilibration run at $T^*=0.470$: P_2 (+); Q_{zz} (×).

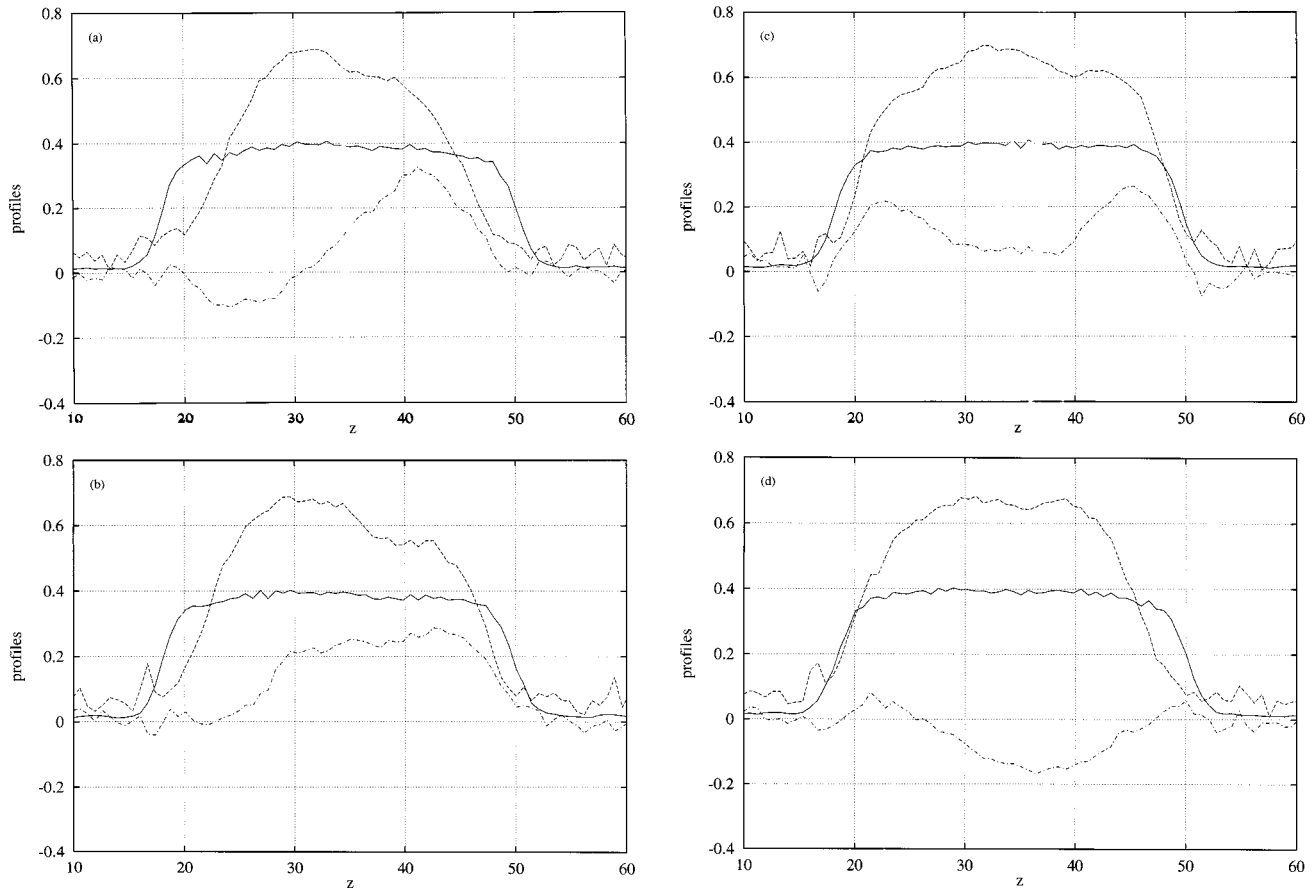

FIG. 12. Subrun-averaged profiles at $T^*=0.470$: $\langle\rho(z)\rangle_{\rm sub}$ (solid line); $\langle P_2(z)\rangle_{\rm sub}$ (dashed line); $\langle Q_{zz}(z)\rangle_{\rm sub}$ (dash-dot line). The z coordinate is in units of σ_0 and the density in units of σ_0^{-3}. Each graph was constructed using data from successive configurations covering 50 000 simulation steps.

center before propagating towards the interfaces, at which they disperse.

To demonstrate this process, we present (Figs. 12) subrun averages of the $P_2(z)$ and $Q_{zz}(z)$ profiles for $T^*=0.470$. Compiled over relatively small time periods (50 000 time steps) for consecutive stages of the production run at this temperature, these show the existence of different nematic domains as regions with similar $\langle Q_{zz}(z)\rangle_{\rm sub}$ values, with changes in the value of $\langle Q_{zz}(z)\rangle_{\rm sub}$ corresponding to the twist that is adopted by the film between these domains. The sequence of profiles here [Figs. 12(a)–12(d)] show an initial two domain arrangement, with a gradual spatial reorientation occurring between the domains. In profile (b), the right-hand domain can be seen to have grown significantly, while profile (c) shows that it goes on to split in two. The final profile shows that these domains of positive Q_{zz} then disperse as the center of the film develops a tilted domain. Orientational fluctuations of this type were observed to occur continually at these intermediate temperatures.

We note that the corresponding $\langle P_2(z)\rangle_{\rm sub}$ profiles [also Figs. 12(a)–12(d)] are relatively insensitive to the domain boundaries (note that in calculating these, only the particles within the relevant slice are considered, so the effects of any gradients in the director are not included directly). However, they do all show a relative disordering at the liquid-vapor interface. The density profiles, $\langle\rho(z)\rangle_{\rm sub}$ are virtually independent of the changing orientational domain structure. The runs we have performed in this study have proved too short to enable a full analysis of this multidomain structure based on orientational time correlation functions. We shall, however, return to this in a future publication.

2. Orientational correlations

On cooling through the intermediate temperature regime, two trends are apparent from animations: (i) an increase in the size and lifetime of the nematic domains formed; (ii) a decrease in the thickness of the disordered interfacial regions. In an attempt to provide a more satisfactory measure of the former, we have calculated the correlations between the instantaneous nematic directors $\hat{\mathbf{d}}(z)$ for each slice of the liquid film (as calculated in the $P_2(z)$ routine). Designated $D_2(z)$, this is formally expressed as

$$D_2(\delta z)=\langle P_2(\hat{\mathbf{d}}(z)\cdot\hat{\mathbf{d}}(z\pm\delta z))\rangle', \tag{7}$$

where the prime on the angled brackets denotes an average restricted to the slices within the liquid region of the film.

The behavior of $\langle D_2(\delta z)\rangle$ for various temperatures around the ordering transition is shown in Fig. 13. For the highest temperature shown, $T^*=0.500$, $\langle D_2(\delta z)\rangle$ quickly decays to zero and the system is clearly isotropic. Correspondingly, at the lowest temperature shown, $T^*=0.450$, $\langle D_2(\delta z)\rangle$ decays slowly, leveling out at a value of approxi-

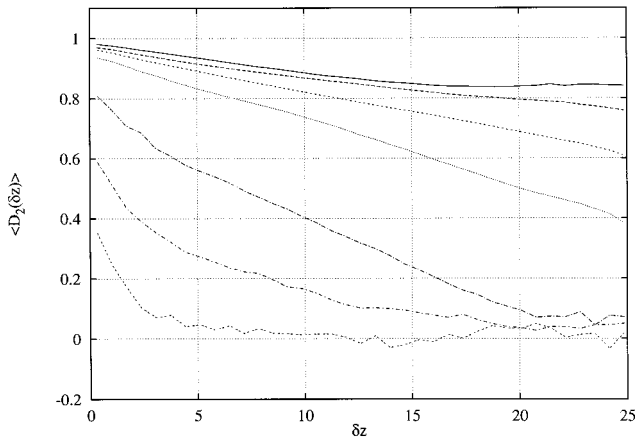

FIG. 13. Layer-layer orientational correlation function, $\langle D_2(\delta z)\rangle$, for a range of temperatures. From top to bottom: $T^*=0.450$, 0.460, 0.465, 0.470, 0.473, 0.475, 0.500. The δz coordinate is in units of σ_0.

mately 0.85, at $\delta z \simeq 15\sigma_0$. The phase present at this temperature has already been identified as being a nematic monodomain. At the other temperatures shown, $\langle D_2(\delta z)\rangle$ drops approximately linearly with δz, only leveling off in the cases where it drops all the way to zero. This slow decay in orientational correlations is not consistent with that seen in simulations of bulk systems, suggesting that the disordering interfaces present in this system strongly modify the ordering process. The behavior of $\langle D_2(\delta z)\rangle$ at larger values of δz can only be examined using thicker films; investigations into the effect of film thickness upon these correlations are presently being undertaken.

A more rigorous estimate of the degree of nematic order in a system is given by the second rank orientational pair correlation function

$$g_2(r)=\frac{\Sigma_{ij}P_2(\hat{\mathbf{u}}_i\cdot\hat{\mathbf{u}}_j)\,\delta(r_{ij}-r)}{\Sigma_{ij}\delta(r_{ij}-r)}, \tag{8}$$

where the molecules i and j are separated by a distance r_{ij}. In the isotropic phase, $g_2(r)$ decays to zero at large r, whereas in the nematic phase it levels out at a value equal to the square of P_2. As an extra measure of the nematic order across the film the system was divided into 20 slices at regular z values and $g_2(r)$ calculated for each slice [i.e., the sums in Eq. (8) were restricted to pairs of particles within the appropriate slice]. This gave the function $g_2(r,z)$, where r is the particle-particle separation, and z is the location of the slice within the film. The number of slices was restricted to 20 in order to obtain reasonable statistics. The $\langle g_2(r,z)\rangle$ data are shown as surface plots [Figs. 14(a)–14(d)] for $T^*=0.475$, 0.473, 0.470, 0.450. At higher temperatures, $\langle g_2(r,z)\rangle$ was found to decay rapidly to zero at all z, indicating a film of isotropic liquid.

At the highest temperature shown, $\langle g_2(r,z)\rangle$ decays to values slightly greater than zero in the middle of the film, corresponding to a small degree of central nematic order (as seen previously in the order parameter profiles). This effect is more noticeable at $T^*=0.473$, where the magnitude of the limiting value is higher and the width of the ordered region is increased. At $T^*=0.470$ this ordering has spread nearly to

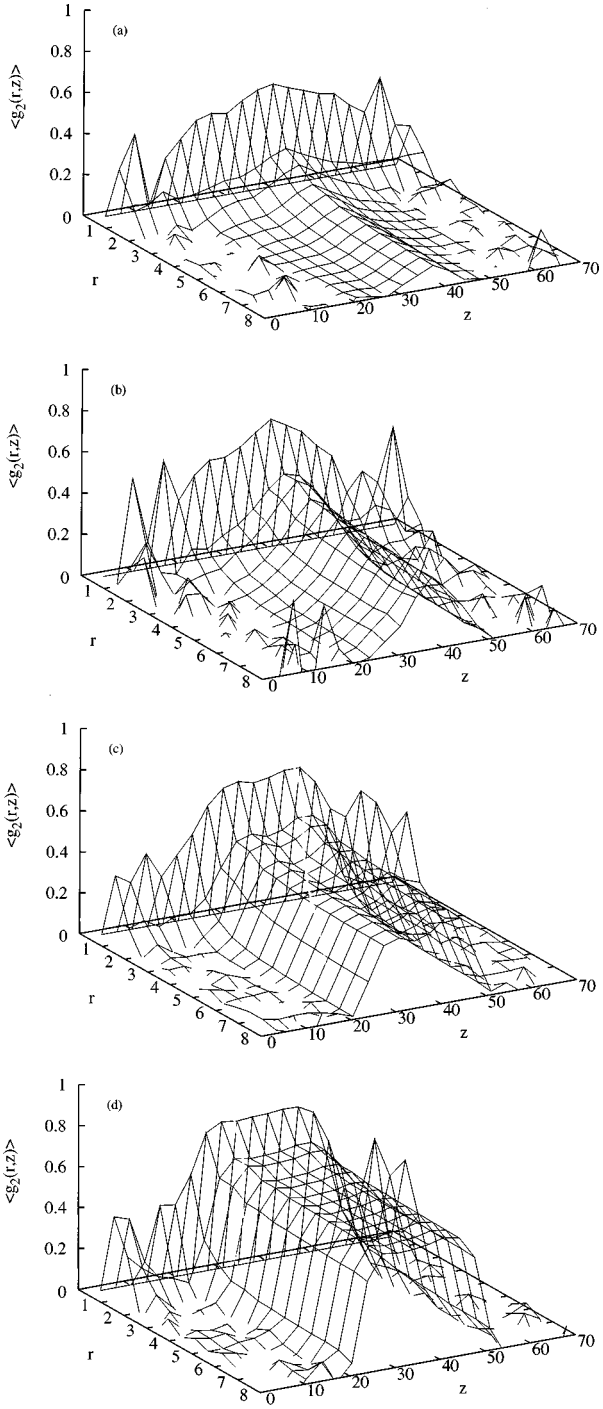

FIG. 14. Surface plots of $\langle g_2(r,z)\rangle$ resolved within layers z for a range of temperatures: (a) $T^*=0.475$; (b) $T^*=0.473$; (c) $T^*=0.470$; (d) $T^*=0.450$. The δz and r coordinates are in units of σ_0.

the edge of the film, but is not quite as wide and is much less sharply defined than the equivalent data obtained for the nematic monodomain at $T^*=0.450$.

Since it is calculated in thin slices, $\langle g_2(r,z)\rangle$ provides a useful measure of the degree of ordering *parallel* to the interfaces. From Fig 14(c) it can be seen that for $T^*=0.470$ that this parallel ordering is reasonably stable, $\langle g_2(r,z)\rangle$ leveling out across much of the film. By contrast, however, $\langle D_2(\delta z)\rangle$ at this same temperature (Fig. 13) indicates that orientational correlations *normal* to the interface continue to

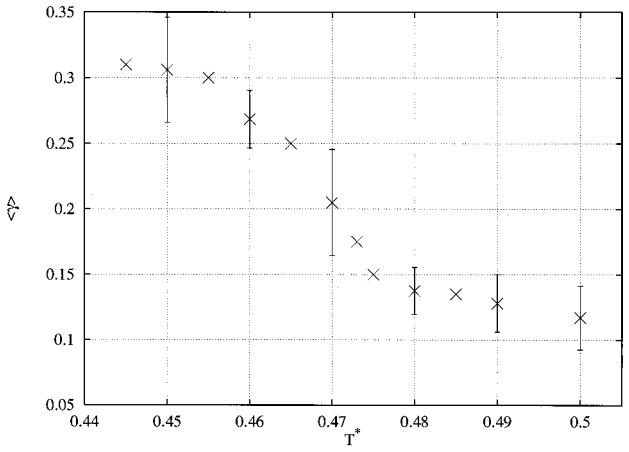

FIG. 15. Run-averaged surface tension $\langle\gamma\rangle$ values over a range of temperatures (error bars shown for certain temperatures). The surface tension is in units of ϵ_0/σ_0^2.

decay at large δz. Indeed, the behavior of $\langle D_2(\delta z)\rangle$ suggests that nematiclike orientational correlations in the z direction develop only for $T^* \leqslant 0.450$. This marked difference between the transverse and longitudinal orientational correlations is presumably due to the symmetry breaking effect of the interfaces. It appears that high temperature nematic growth is stabilized by the in-plane periodicity of the system. Longitudinal correlations, conversely, are less easily established due to the inherently disordered interfaces: hence the domains of nematic order formed through strong transverse correlations fail to spread throughout the system. Only at temperatures sufficiently low to stabilize orientational order at the interfaces does the system become nematic in all three dimensions.

3. Surface tension

The surface tension values calculated for each temperature are shown in Fig. 15. Error bars are shown at temperature intervals of 0.1. The values in the vapor-isotropic ($0.480 \leqslant T^* \leqslant 0.520$) and vapor-nematic ($0.445 \leqslant T^* \leqslant 0.460$) regions show the expected inverse correlation with temperature, with $\langle\gamma\rangle$ decreasing linearly as the temperature is increased and the surfaces become less rigid. As orientational order grows, a large increase in $\langle\gamma\rangle$ is observed, consistent with theoretical predictions for surface disordering systems [8,23]. The temperature dependence of the rapid rise in $\langle\gamma\rangle$ closely matches that of the nematic order parameter $\langle P_2\rangle$. Thus, we note that the film's overall surface tension is considerably enhanced even at temperatures (e.g., $T^* = 0.470$) for which there is little or no orientational order *at* the liquid-vapor interface. This enhancement is presumably due to the additional N-I interfaces (along with any nematic-nematic ones) present at these temperatures. While theoretical treatments of this situation attribute the jump from the I-V to the N-V branches of the surface tension to such additional interfaces, it cannot be used to measure γ_{NI} directly; a fuller picture of the wetting behavior (partial or complete) displayed by the system is needed first. We are currently conducting simulations of different system sizes in order to clarify this situation.

As well as showing the expected temperature dependence our surface tension data compare well with the values obtained in the GB thin film simulations of Martin del Rio and De Miguel [27]. The $\langle\gamma_{IV}\rangle$ values reported here are slightly lower (0.05–0.15, c.f. 0.15–0.25) but this is to be expected since shorter molecules will lead to less rigid interfaces. For $\langle\gamma_{NV}\rangle$, the difference is very small (approximately 0.3, c.f. 0.25–0.35); what is more noticeable is that the gradient of $\langle\gamma_{NV}\rangle$ with respect to temperature is much smaller for our perpendicularly aligned surface system (-1.3, c.f. -5).

IV. CONCLUSIONS

We have performed a detailed simulation study of a GB system with free interfaces that shows perpendicular alignment and isotropic wetting of the nematic phase. Since the interfaces are the only symmetry breaking aspect of the system, the director alignment must be induced by them. This is supported by the observation that this alignment is selected only once the nematic ordering has reached the liquid-vapor interfaces. The phase behavior exhibited by the system has proved consistent with the results obtained from GEMC simulations, a small negative shift in the ordering transition temperature being attributable to the observed surface disordering.

The wetting behavior has been established both from direct observation that nematic order develops preferentially at the center of the film and indirectly from the temperature dependence of the surface tension. At intermediate temperatures, where central nematic domains coexist with disordered interfacial regions, there is weak evidence of a tendency for the central regions to tilt with respect to the liquid-vapor interfaces. We note that this is consistent with results from a recent GB simulation [37] of a N-I interface in which parallel alignment was observed. Experimental results have demonstrated that numerous systems exhibit different induced orientations at the N-I and N-V interfaces, for example, 5, 6, 7, and 8 CB show tilted orientation at the isotropic interface [38] and perpendicular at the vapor surface [18]. Theoretical work also predicts such effects, showing that they result from competition between the parallel and perpendicular ordering terms [6]. However, our measurements of director orientation within the central nematic domains indicate considerable fluctuations along with rather diffuse N-I interfaces. The slight evidence we have of a tilt may, therefore, simply be due to the inherently slow process of domain formation and dispersion through which the orientational order manifests itself in this regime. The dominant arrangement at these temperatures is one of several competing nematic domains occupying a region centered upon the film's midline and bounded on both sides by disordered liquid. Only on cooling to the point where the liquid-vapor interfaces become ordered is there a straightforward situation in which an orientationally pinned nematic monodomain remains stable.

It seems reasonable to conclude that the preferred orientation at the free interface is determined by the relative well depths of the various interactions possible, these being ultimately controlled by the parametrization used. Naive arguments, based on the relative energies of various cleavage planes for close-packed structures, suggest that the ratio κ/κ' (recall that κ is the length to breadth ratio, while κ' is

the well-depth ratio for side-side and end-end arrangements) should provide a good indication of the prefered alignment; it should be parallel if κ/κ' is greater than unity, but perpendicular if it drops below this threshold. Whilst these arguments neglect the liquid nature of the phases formed, they are consistent with all published simulation data: parallel alignment was obtained using $\kappa=3.0$, $\kappa'=1.0$ [27,28]; an earlier study [39] of the liquid-vapor interface using the standard GB parameterization ($\kappa=3.0$, $\kappa'=5.0$) hinted at perpendicular alignment at the free interface, without showing nematic-vapor coexistence and the model used here ($\kappa=2.0$, $\kappa'=5.0$) definitely shows perpendicular alignment.

The wetting behavior is also affected by the parametrization used, showing perhaps a greater dependency upon the shape anisotropy κ. Whereas isotropic wetting has been observed here with $\kappa=2.0$, the parallel alignment simulations saw nematic wetting with more elongated particles, $\kappa=3.0$. This is consistent with theoretical predictions showing a crossover from isotropic to nematic wetting with increase in anisotropy [6] and experimental observations of the cyanobiphenyls, which show an increase in nematic wetting ability with increasing molecular length.

Also, the influence of μ and ν on the interaction well depths and, subsequently, the phase behavior cannot be ignored. We note, in passing, that simulations of *confined* GB systems suggest that μ and ν are crucial in determining the arrangement of the transition region that couples the bulk liquid crystal to the underlying substrate. For example, the standard GB parameterization ($\kappa=3.0,\kappa'=5.0$) has repeatedly shown itself unable to yield bulk alignment orthogonal to a substrate, although orthogonal alignment in the interfacial layer is easily obtained [40]. Unfortunately, systematic characterization of the effect of μ and ν on the behavior at the free surface is more difficult than would be first thought, since nematic-vapor coexistence is only observed for a very restricted range of parametrizations. A primary cause of this appears to be the relative depth of the side-side interaction: if this is made too deep (e.g., due to high shape anisotropy, or inappropriate choice of the exponents μ and ν) the isotropic-nematic-smectic triple point temperature goes above that of the liquid crystal-isotropic-vapor triple point and the only liquid crystal-vapor coexistence possible is with the smectic phase. However, fine tuning of the parameters, subject to careful control of this well-depth, should enable further nematic-vapor coexistence regions to be located and thus clarify the effects of the various parameters upon the surface phase behavior. Particularly attractive would be an attempt to observe a switch from perpendicular to planar or even oblique alignment by using intermediate values of κ'; though the fluctuation effects observed here are likely to prove even more of a problem in such a system (it would have to establish a common azimuthal angle at both interfaces), and its satisfactory equilibration would present a considerable challenge.

ACKNOWLEDGMENTS

We would like to thank G. D. Wall for his assistance with this work. We gratefully acknowledge the financial support of DERA Malvern and the MRI in providing a bursary for S.J.M. This work has been performed on computational hardware provided under Grant No. GR/K11956 from the U.K. EPSRC.

[1] P. Sheng, Phys. Rev. A **26**, 1610 (1982).
[2] A. Poniewierski and T. J. Sluckin, Liq. Cryst. **2**, 281 (1987).
[3] B. Jérôme, Rep. Prog. Phys. **54**, 391 (1991).
[4] M. M. Telo da Gama, Mol. Phys. **52**, 585 (1984); J. M. Thurtell, M. M. Telo da Gama, and K. E. Gubbins, *ibid.* **54**, 321 (1984).
[5] B. Tjipto-Margo, A. K. Sen, L. Mederos, and D. E. Sullivan, Mol. Phys. **67**, 601 (1989).
[6] E. Martin del Rio, M. M. Telo da Gama, E. De Miguel, and L. F. Rull, Phys. Rev. E **52**, 5028 (1995).
[7] M. M. Telo da Gama, in *Observation, Prediction and Simulation of Phase Transitions in Complex Fluids*, Vol. 460 of *NATO Advanced Study Institute, Series C: Mathematical and Physical Sciences*, edited by M. Baus, L. F. Rull, and J. P. Ryckaert (Kluwer, Dordrecht, 1995), pp. 243–292.
[8] Y. Martinez-Raton, E. Velasco, A. M. Somoza, L. Mederos, and T. J. Sluckin, J. Chem. Phys. **108**, 2583 (1998).
[9] B. Tjipto-Margo and D. E. Sullivan, J. Chem. Phys. **88**, 6620 (1988).
[10] J. G. Gay and B. J. Berne, J. Chem. Phys. **74**, 3316 (1981).
[11] G. R. Luckhurst and P. S. J. Symmonds, Mol. Phys. **80**, 233 (1993).
[12] J. D. Parsons, Mol. Phys. **42**, 951 (1980); P. Harrowell and D. W. Oxtoby, *ibid.* **54**, 1325 (1985).
[13] B. J. Berne and P. Pechukas, J. Chem. Phys. **56**, 4213 (1972).
[14] E. Martin del Rio, M. M. Telo da Gama, E. De Miguel, and L. F. Rull, Europhys. Lett. **35**, 189 (1996).
[15] M. A. Bouchiat and D. Langevin-Cruchin, Phys. Lett. **34A**, 331 (1971).
[16] P. Chiarelli, S. Faetti, and L. Fronzoni, J. Phys. (Paris) **44**, 1061 (1983).
[17] P. Chiarelli, S. Faetti, and L. Fronzoni, Phys. Lett. **101A**, 31 (1984).
[18] H. Kasten and G. Strobl, J. Chem. Phys. **103**, 6768 (1995).
[19] J. Als-Nielsen, F. Christensen, and P. S. Pershan, Phys. Rev. Lett. **48**, 1107 (1982).
[20] V. A. Korjenevsky and M. G. Tomilin, Liq. Cryst. **15**, 643 (1993).
[21] R. Lucht and Ch. Bahr, Phys. Rev. Lett. **78**, 3487 (1997); **80**, 3783 (1998); R. Lucht *et al.*, J. Chem. Phys. **108**, 3716 (1998).
[22] S. Krishnaswamy and R. Shashidhar, Mol. Cryst. Liq. Cryst. **35**, 253 (1976).
[23] M. M. Telo da Gama, Physica A **244**, 389 (1997).
[24] G. R. Luckhurst, T. J. Sluckin, and H. B. Zewdie, Mol. Phys. **59**, 657 (1986).
[25] M. M. Telo da Gama, P. Tarazona, M. P. Allen, and R. Evans, Mol. Phys. **71**, 801 (1990).
[26] D. J. Cleaver and M. P. Allen, Mol. Phys. **80**, 253 (1993).
[27] E. Martin del Rio and E. De Miguel, Phys. Rev. E **55**, 2916 (1997).

[28] A. P. J. Emerson, S. Faetti, and C. Zannoni, Chem. Phys. Lett. **271**, 241 (1997).
[29] E. De Miguel, E. Martin del Rio, J. T. Brown, and M. P. Allen, J. Chem. Phys. **105**, 4234 (1996).
[30] G. R. Luckhurst, R. A. Stephens, and R. W. Phippen, Liq. Cryst. **8**, 451 (1990).
[31] E. De Miguel, L. F. Rull, M. K. Chalam, and K. E. Gubbins, Mol. Phys. **74**, 405 (1991).
[32] J. T. Brown, M. P. Allen, E. Martin del Rio, and E. De Miguel, Phys. Rev. E **57** 6685 (1998).
[33] A. P. J. Emerson and C. Zannoni, J. Chem. Soc., Faraday Trans. **91**, 3441 (1995).
[34] See, e.g., A. Z. Panagiotopoulos, Mol. Phys. **62**, 701 (1987); A. Z. Panagiotopoulos, N. Quirke, M. Stapleton, and D. J. Tildesley, *ibid.* **63**, 527 (1988).
[35] R. Eppenga and D. Frenkel, Mol. Phys. **53**, 1303 (1984); G. D. Wall and D. J. Cleaver, Phys. Rev. E **56**, 4306 (1997).
[36] A. Harashima, Adv. Chem. Phys. **1**, 203 (1958).
[37] M. A. Bates and C. Zannoni, Chem. Phys. Lett. **280**, 40 (1997).
[38] S. Faetti and V. Palleschi, Phys. Rev. A **30**, 3241 (1984).
[39] E. Martin del Rio, E. De Miguel, and L. F. Rull, Physica A **213**, 138 (1995).
[40] M. K. Challam, K. E. Gubbins, E. De Miguel, and L. F. Rull, Mol. Simul. **7**, 357 (1991); T. Gruhn and M. Schoen, Mol. Phys. **93**, 681 (1998); V. Palermo, F. Biscarini, and C. Zannoni, Phys. Rev. E **57**, R2519 (1998).